

INVESTIGATION OF IRON LOSSES IN A HIGH FLUX INTERIOR PM AUTOMOTIVE ALTERNATOR

V. Zivotic-Kukulj, W.L. Soong and N. Ertugrul
University of Adelaide

Abstract

This paper examines the iron loss characteristics of a high-flux interior PM machine. This was designed as a concept demonstrator for a 6kW automotive alternator and has a wide field-weakening range. Initial experimental tests showed a high iron loss during high-speed field-weakening conditions. This paper examines the causes of this high iron loss using finite-element simulations and experimental tests. It was found that the high iron loss was due to high harmonic airgap flux density components during field-weakening. Means to reduce these losses are discussed.

1 INTRODUCTION

Proposed new features in cars such as active suspension systems, electric air-conditioning and sophisticated electronic controls have meant that the existing automotive alternator cannot satisfy the growing electrical power demands.

A proposed specification for a high power alternator is a linearly increasing output power from 4kW to 6kW as the engine speed increase from idle (600rpm) to maximum operating speed (6krpm) [1]. Figure 1 shows the output power specification versus alternator speed assuming a 3:1 belt ratio between the alternator and engine. This challenging requirement requires a 10:1 constant power speed range. Interior permanent magnet (PM) machines are one of the few machine types capable of delivering such a wide constant power speed range.

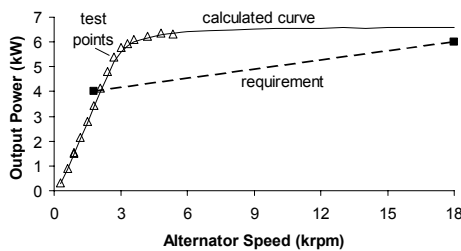


Figure 1. Output power characteristics of the interior PM alternator showing the measured performance (triangles) versus the calculated performance (lines) at rated voltage. The high power alternator specification is also shown [1].

An interior PM concept demonstrator for a 6kW automotive alternator was built in [1]. Figure 1 shows the measured and calculated output power characteristics of the interior PM machine showing the potential to meet the high power alternator specification. The experimental results were limited to 6krpm by dynamometer limitations.

The concept demonstrator used a high flux interior PM machine based on rare-earth magnets (NdFeB). The machine was based a commercial 415V, 2.2kW, 4 pole

induction motor stator and used a custom designed rotor which uses three flux-barriers per pole (see Fig. 2). The motor stack length was 95mm, the stator outer diameter was 153mm, the rotor diameter was 92mm, and the airgap was 0.39mm. The rotor uses a number of rounded bridges to mechanically retain the magnets at high speed.

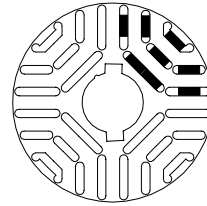


Figure 2. Rotor lamination cross-section [1].

Iron loss during field-weakening operation of interior PM machines has been examined in [2] using time-stepping finite-element analysis. They found that in these machines the iron loss is significant, especially at high speeds. Their finite-element analysis results showed that a significant amount of iron loss is due to high frequency harmonic flux components near the airgap. This is likely to also be the case with the interior PM machine considered in this paper.

The paper is organised as follows : firstly, the experimental obtained machine loss measurements are discussed; secondly, finite-element analysis is used to examine the spatial distribution of the airgap flux density during field-weakening is examined; thirdly, additional measurements on the stator tooth flux waveforms are examined; and finally, motor design methods for reducing the iron loss are discussed.

2 MACHINE LOSS MEASUREMENTS

In this section, experimental loss measurements were taken on the machine to examine the variation of iron losses with speed and operating conditions.

Figure 3 shows the measured efficiency at rated voltage of the interior PM machine corresponding to the output curves shown in Fig. 1. Below 2.5krpm, the

copper losses dominate and they are relatively constant. As the speed increases, so does the output power and hence efficiency. Above 2.5krpm, the output power and copper loss are relatively constant and the drop in efficiency is due to iron losses.

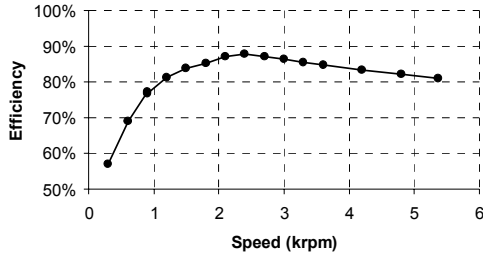


Figure 3. Measured efficiency at rated voltage of the interior PM machine [1].

Figure 4 shows the measured losses for the interior PM machine at rated voltage corresponding to the efficiency plot shown in Fig. 3. The total losses are calculated as the difference between the input and output power at rated voltage. The iron and mechanical (friction/windage) losses are calculated by subtracting the copper losses ($3I^2R$) from the total loss curve. The iron and mechanical losses at one-third rated output voltage are also shown.

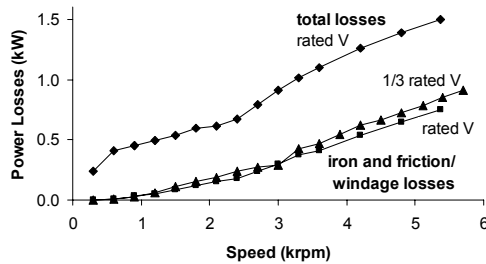


Figure 4. Measured losses for the interior PM machine. The total losses are shown at rated voltage. The iron and friction/windage losses are shown at both rated and one-third rated voltage [1].

At 6krpm, the iron loss and mechanical loss is about 800W. As the outer surface of the rotor is smooth, it is assumed that the majority of this loss is iron loss. Assuming that this loss increases with the square of frequency, this results in an extremely large estimated iron loss of above 7kW at the maximum alternator operating speed of 18krpm.

The iron loss is not significantly affected by the output voltage and hence by the magnitude of the fundamental component of the flux. This shows that the iron losses are likely to be caused by harmonic flux components.

Figure 5 shows the measured iron and mechanical losses as a function of speed under open-circuit and short-circuit conditions [3]. For comparison purposes it also shows the curve in Fig. 4 for losses under rated output voltage.

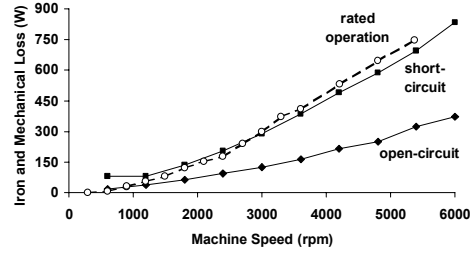


Figure 5. Measured iron and mechanical losses as a function of speed under open-circuit, short-circuit and rated output voltage conditions.

The open-circuit losses were obtained from the input mechanical power ($T\omega$) when driving the machine under open-circuit conditions.

The short-circuit iron and mechanical losses were obtained by subtracting the copper loss from the input mechanical power required when driving the machine with the stator terminals short-circuited. This is sometimes referred to as a forced-running short-circuit test. Under these conditions, the rotor magnets induce currents in the short-circuited stator winding which produces a flux which opposes the rotor magnet flux. At high speeds, ideally the stator and rotor flux should cancel one another, resulting in a small total airgap flux distribution and a low iron loss, or at least an iron loss which remains constant. In practice, Fig. 5 shows that the losses under short-circuit conditions are roughly twice that under open-circuit conditions. This is likely to be due to harmonic flux components as shown in the next section.

In conventional PM machines, it is expected that the rated operation curve in Figure 5 should be very close to the open-circuit curve. This is because the airgap flux produced with rated stator currents is normally much smaller than the airgap flux produced by the rotor magnets. Thus the presence or absence of stator currents should not significantly change the total flux distribution and hence not change the iron losses.

The interior PM machine was designed to operate with a back-emf voltage which is much larger than the output voltage [1]. For instance at 6,000rpm, the open-circuit line back-emf is estimated at 1,084Vrms, while the rated output voltage is 415Vrms, what is about 2.6 times smaller. Under these conditions the machine is effectively operating into a short-circuit and thus the iron losses at rated operation are close to the short-circuit iron losses.

3 FINITE ELEMENT ANALYSIS RESULTS

In this section, finite-element analysis (FEA) is used to examine the airgap flux distribution during open-circuit and field-weakening conditions.

Finite-element analysis provides a convenient means for obtaining the magnetic field distribution for complex electromagnetic geometries taking into

account magnetic saturation. It involves dividing the given machine geometry into thousands of small elements (mostly triangles). Maxwell's equations are then solved for each of these elements to determine the field distribution taking into account the physical properties of each element such as BH characteristics, residual magnetism and current flow. From this field distribution, the stored energy, co-energy and other electrical parameters can be determined. Due to symmetry reasons, only a quarter of the machine has been analysed. The Magsoft Flux2D package was used in the analysis.

As shown in Figure 2, the magnets do not take up entire area of the rotor slots (flux-barriers). The magnets were modelled by reducing the magnet remanent flux density by the ratio of the magnet area to the slot area.

FEA was used to investigate the variation of the airgap flux density distribution to determine the cause of the high iron losses. Four cases were considered : rotor flux only, q-axis stator flux, d-axis stator flux, and a combination of rotor flux and d-axis stator flux simulating field-weakening conditions.

3.1 Rotor PM Flux Distribution

Figure 6 shows a finite-element flux plot and airgap radial flux density graph for the case where there is only rotor magnets and no stator current. The airgap flux density shows a rectangular waveform of peak value approximately 0.7T. The dips in the waveform correspond to the stator slotting. Note that reducing the width of the stator slot openings will reduce the depth of the dips. Figure 6 also shows the fundamental component of the airgap flux waveform (0.666T peak).

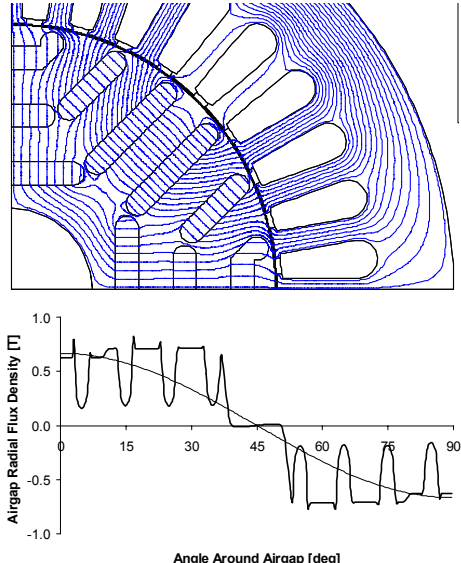


Figure 6. Rotor magnets only. FEA flux plot and airgap radial flux distribution with fundamental component.

3.2 Q-Axis Stator Flux Distribution

Figure 7 shows the flux distribution corresponding to rated q-axis current (9.4A) with a reluctance rotor (no PM). The waveform shows a roughly sinusoidal flux distribution which again is modulated by the stator slotting. The fundamental component has a peak of about 1.03T.

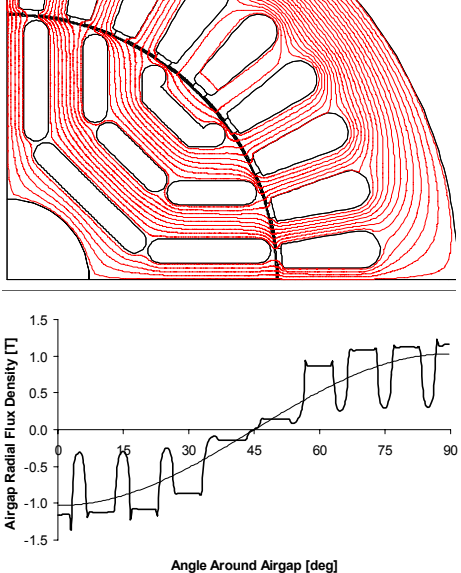


Figure 7. Rated current in q-axis, no magnets. FEA flux plot and airgap radial flux distribution with fundamental component.

3.3 D-Axis Stator Flux Distribution

Figure 8 shows the flux distribution corresponding to rated current (9.4A) in the d-axis.

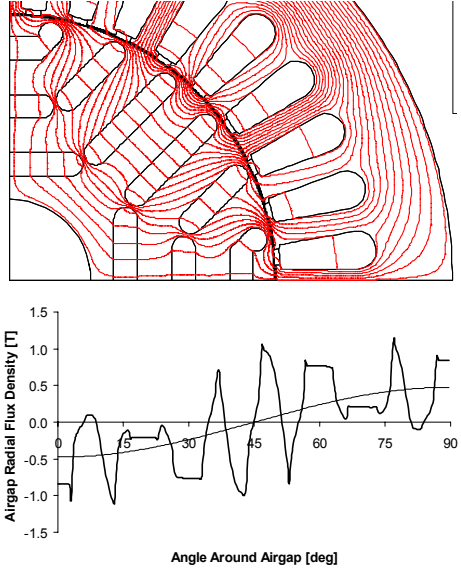


Figure 8. Rated current in d-axis, no magnets. FEA flux plot and airgap radial flux distribution with fundamental component.

The waveform shows the presence of high frequency spatial harmonics. These harmonics are caused by

interactions between the stator and rotor slotting. This interaction results in zig-zag leakage flux which occurs when stator flux crosses the airgap to the rotor and then returns to the stator without passing through the rotor flux-barriers. This is especially evident near 45° . The waveform has a fundamental component of 0.476T.

3.4 Rotor Flux and D-Axis Stator Flux Distribution

Figure 9 shows the flux distribution with rated demagnetising stator current in the d-axis (9.4A) and with rotor magnets. The airgap flux density waveform is nearly the sum of the waveforms from Figure 6 and 8. The fundamental component of the airgap flux density waveforms with only rotor magnets is 0.666T (Figure 6) and with rated d-axis stator current is 0.476T (Figure 8). Thus the expected fundamental component of the sum of the two opposing fields is 0.190T, while the actual sum from Figure 9 is 0.224T. The small difference is likely to be due to magnetic saturation.

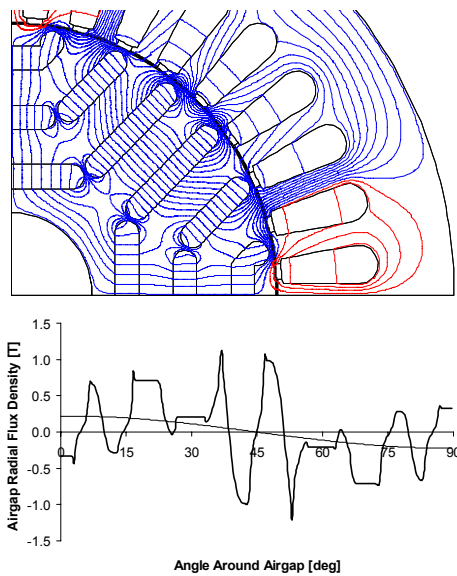


Figure 9. Rated current in d-axis with rotor magnets. FEA flux plot and airgap radial flux distribution with fundamental component.

The value of rated current used (9.4A) is that required to reduce the fundamental component of the stator voltage to zero at the stator terminals. The rated current was chosen to be equal to the forced-running short-circuit current at high speeds. It does not correspond to zero airgap fundamental flux because of the finite leakage inductance (slot-leakage and end-winding) of the machine.

Iron losses are associated with time variations in flux density and so in the next section the time-varying machine flux distribution is investigated to see whether these high harmonic spatial flux components

results in high harmonic time-varying flux components in the machine.

4 IRON LOSS MEASUREMENTS

The majority of iron losses in synchronous machines normally occurs in the stator, as ideally the rotor does not see a changing magnetic field. To better understand the stator losses, the stator tooth magnetic flux variation versus time was examined using a search coil wound around a stator tooth.

The eddy-current loss component of the iron losses in a magnetic material are proportional to the time average of the square of the rate of change of magnetic flux density (dB/dt). As the induced voltage in the search coil is proportional to dB/dt , thus the eddy-current iron loss is proportional to the mean square value of the induced search coil voltage.

To obtain the stator tooth flux associated with the airgap flux, it is important to insert search coil as close as possible to the airgap. The location of the search coil is illustrated in Figure 10.

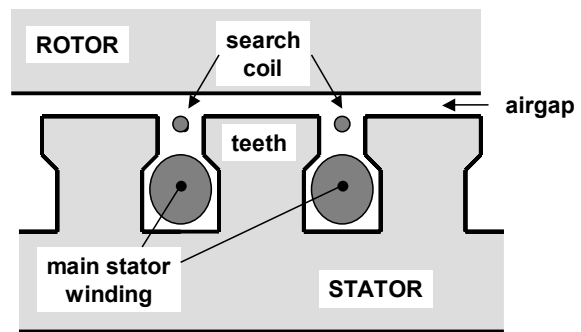


Figure 10. Diagram showing the location of the search coil. The search coil covers a single stator tooth and consists of five turns of fine wire. The stator tooth flux waveform was obtained by integrating the search coil induced voltage. This was performed using a resistor-capacitor low-pass filter whose cut-off frequency of 5Hz is much lower than (one tenth of) the 50Hz fundamental frequency.

The stator tooth flux waveform was examined for three cases : q-axis stator currents only, rotor magnets only, and the combination of d-axis stator currents and rotor magnets corresponding to field-weakening operation. Unfortunately it was not possible to obtain the d-axis current results.

4.1 Q-Axis Stator Currents

The first search coil measurements were performed by replacing the interior PM rotor with a squirrel-cage induction motor rotor and testing the machine with no mechanical load. Under these conditions, the slip and hence the rotor currents are negligible and hence the rotor field is zero. Thus the machine acts like it has a round rotor and the flux in the machine is purely due to the stator field.

Figure 11 shows the induced voltage in the search coil and the corresponding stator tooth flux waveform corresponding to the above case with rated stator voltage. The flux waveform (lower) is roughly sinusoidal but shows some saturation at its peak.

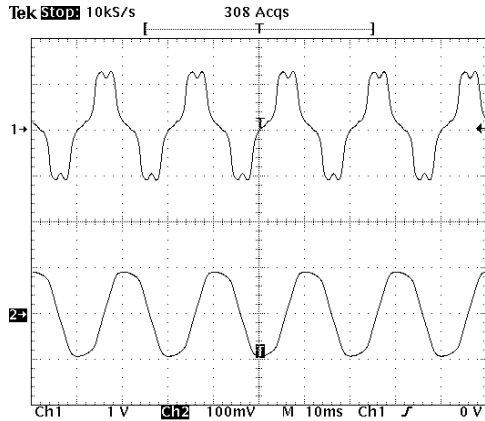


Figure 11. Stator flux only. Search coil induced voltage (upper) and corresponding stator tooth flux waveform (lower) at 1,500rpm.

4.2 Rotor Magnet Only

Figure 12 shows the search coil voltage and the stator tooth flux waveform for the interior PM rotor with the stator windings open-circuited. The flux waveform is roughly rectangular and shows a significant asymmetry. This is likely to be due to an asymmetry in either the magnetisation or location of the magnets in the four poles of the rotor. The induced voltage in the search coil was about 0.79Vrms.

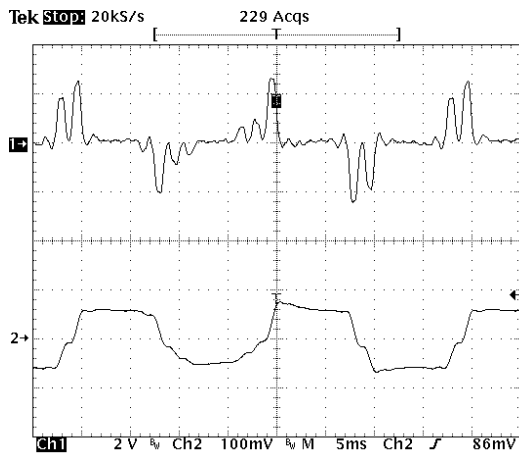


Figure 12. Rotor flux only. Search coil induced voltage (upper) and corresponding stator tooth flux waveform (lower) at 1,500rpm.

4.3 D-Axis Stator Currents and Rotor Magnets

Figure 13 was obtained by short-circuiting the stator and spinning the PM machine at 1,500rpm. The induced currents in the stator will produce a flux which try to cancel the rotor magnet flux. Ideally the airgap flux should be zero at high speeds.

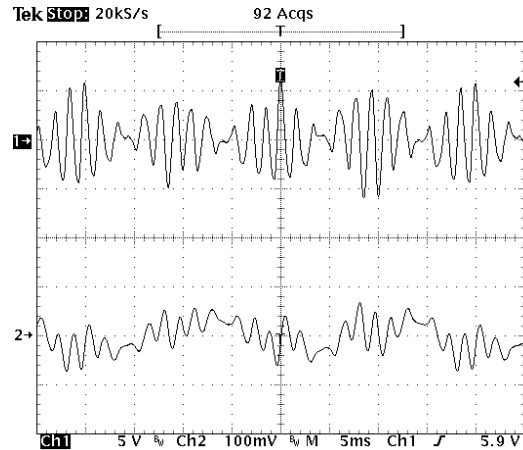


Figure 13. Stator and rotor flux at short-circuit operation at 1,500rpm. Search coil induced voltage (upper) and corresponding stator tooth flux waveform.

Figure 14 shows the same waveforms as in Figure 13, but for a lower speed operation of 375rpm. At lower speeds the effect of stator resistance reduces the demagnetising d-axis current and hence Figure 13 shows a much larger fundamental flux component and slightly lower amplitude harmonic flux components.

Comparing the two cases reveals that the fundamental component of the flux and the amount higher frequency harmonics is much larger at lower speeds.

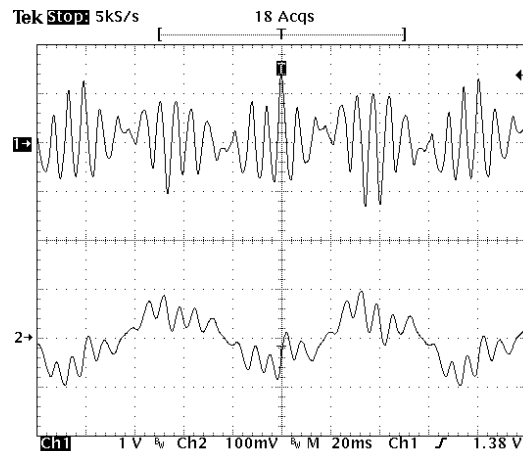


Figure 14. Stator and rotor flux at short-circuit operation at 375rpm. Search coil induced voltage (upper) and corresponding stator tooth flux waveform.

As indicated earlier, the eddy-current losses are proportional to the mean square of the search coil voltage. The root mean square (rms) search coil induced voltage at 1,500rpm under open-circuit conditions (Figure 12) is 0.79V, while for the short circuit case (Figure 13) is 2.38V giving a ratio of about 3. This implies that the stator tooth eddy-current losses under short-circuit conditions would be expected to be nine times that under open-circuit conditions. This dramatic increase in stator tooth iron losses is likely to a key factor in the doubling of the

total iron losses going from open-circuit to short-circuit conditions shown in Figure 5.

Figure 15 shows the rms induced voltage measurements as a function of speed showing that the ratio between the two cases is roughly constant except at very low speeds.

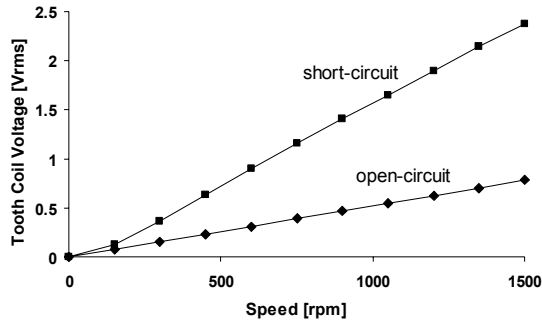


Figure 15. RMS search coil voltages as a function of speed for the open-circuit and short-circuit tests.

5 DESIGN CONSIDERATIONS

The above results have shown that the high iron loss is due to large amplitude, higher harmonic airgap flux components. Means for reducing these include :

- using lower loss lamination material : the interior PM machine uses a low-cost commercial 50Hz induction motor stator despite the high expected fundamental frequency (200Hz at 6,000rpm). Using higher quality lamination material should provide an immediate significant reduction in iron loss.
- number of rotor barriers : for synchronous reluctance machines, a design recommendation to reduce iron losses is that the number of rotor slots should equal the number of stator slots in order to minimise the stator and rotor tooth flux variations as the rotor rotates [4]. In order to implement this would require adding additional flux-barriers to the rotor.
- optimisation of the rotor magnet flux distribution : the amount of magnets in each flux-barrier could be optimised to produce a more sinusoidal airgap magnet flux distribution.
- stator winding design : the existing stator uses a single-layer winding. A double-layer may provide more sinusoidal stator flux density distribution.
- stator slot opening : increasing the stator slot opening will reduce the zigzag flux component but reduce the q-axis inductance.

6 CONCLUSIONS

This paper has used finite-element and measured stator tooth flux waveforms in order to investigate the cause of the high iron losses in a 6kW interior PM alternator.

The key results are as follows :

- the measured iron losses under field-weakening conditions are similar to the losses under forced-running short-circuit conditions, and they are approximately double the magnitude of the open-circuit losses,
- finite-element analysis has shown that spatial airgap flux density waveform under field-weakening conditions shows a low fundamental frequency component but very high spatial harmonic frequency components,
- measurements of stator tooth flux waveforms using a search coil showed that under forced-running short-circuit conditions there are high amplitude, high frequency time harmonic components.

The results thus indicate that the high iron loss in this machine during field-weakening is due to large amplitude, higher harmonic flux components particularly caused by the high permanent magnet rotor flux and high stator currents used in this machine.

Future work involves the optimisation of the machine design to reduce these losses. We will consider techniques such as : varying the number and placement of rotor barriers, altering the size of the stator slot openings, using lower loss magnetic materials, and varying the stator winding design.

ACKNOWLEDGMENT

This work was supported by a University of Adelaide scholarship and a 2003 Australian Research Council Discovery Grant. Technical support from the School of Electrical and Electronic Engineering's mechanical workshop and from G. Liew and C.Z. Liaw is gratefully acknowledged.

REFERENCES

- [1] W.L. Soong and N. Ertugrul, "Inverterless High Power Interior Permanent Magnet Alternator", IEEE Industrial Applications Society Annual Meeting, 2003, pp. 1405-1412.
- [2] B. Stumberger and A. Hamler, "Analysis of Iron Loss in Interior Permanent Magnet Synchronous Motor Over a Wide-Speed Range of Constant Output Power Operation", IEEE Transactions on Magnetics, 2000, vol. 36, no. 4, pp. 1846-1849.
- [3] C.Z. Liaw, D.M. Whaley, W.L. Soong and N. Ertugrul, "Investigation of Inverterless Control of Interior Permanent Magnet Alternators," IEEE Industrial Applications Society Annual Meeting, 2004 (to be published).
- [4] T.A. Lipo, A. Vagati, L. Malesani and T. Fukao, "Synchronous Reluctance Motors and Drives – A New Alternative," IEEE Industrial Applications Society Annual Meeting Tutorial, 1992, pp 2-15.